ADVANCED OPTICAL MATERIALS
www.advopticalmat.de

Fundamental Performance Limits and Haze Evaluation of Metal Nanomesh Transparent Conductors

*Tongchuan Gao, Sajad Haghanifar, Maxwell G. Lindsay, Ping Lu, Md Imrul Kayes, Bradley D. Pafchek, Ziyu Zhou, Paul R. Ohodnicki, and Paul W. Leu**

Metal nanomeshes are demonstrated as flexible transparent conductors with performance comparable to indium tin oxide. However, it is not known what the performance limits of these structures are in terms of transparency and sheet resistance. More importantly, the haze, which describes how much incident light is scattered by these structures, has not been studied. In this paper, the transmission, sheet resistance, and haze of metal nanomeshes are comprehensively studied to determine their fundamental performance limits as transparent conductors through simulations and experiments. Numerical simulations and analytical calculations are used to evaluate the tradeoffs and correlations between these three figures of merit. A strong correlation is found between haze and transmission, where structures with high transmission tend to have low haze and vice versa. Structures with a pitch above 1000 nm are beneficial for achieving transmission over 80% and larger thickness is favorable in reducing sheet resistance without significantly affecting transmission. Furthermore, metal nanomeshes are fabricated to verify simulation results. The haze may be primarily explained by Fraunhofer diffraction, but the spectral dependence of haze requires analysis with Mie scattering theory. The results should apply to all metal grid or grating-like structures. The fundamental performance limits evaluated here are helpful for guiding engineering design and research prioritization.

1. Introduction

Transparent conductors are an important component in a variety of optoelectronic applications,such as solar cells,[1] displays, touch screens, and light-emitting diodes.[2] Recently, many inexpensive and alternative flexible transparent conductors have been demonstrated, including metal nanowires,[3] metal grids and nanomeshes,[4,5] carbon-based materials,[6] and various hierarchical structures.[7,8] Many of these alternative transparent conductors have demonstrated comparable or superior performance to indium tin oxide (ITO) in terms of optical transmission and sheet resistance. Most research on alternative transparent conductors has focused on evaluating and understanding the performance limits and tradeoffs in terms of optical transmission and sheet resistance, such as studies on metal nanowire films.[9,10] However, aside from these two figures of merit, haze, which describes the amount of transmitted light that is scattered, is another important figure of merit for transparent conductors that has largely been unstudied. Haze is a critical factor in the light management for a variety of optoelectronic devices. In solar cells, for instance, considerable power conversion efficiency loss is attributed to the light that fails to couple into the photoactive layers, due to the reflection at interfaces.[11] Implementing transparent conductors with high haze as the top electrode may diminish such loss by increasing the absorption of light that enters the solar cell. Similarly, incorporating high haze substrates into organic light-emitting diodes may lead up to 20% improvement in luminescent efficacy.[12] In contrast, applications such as flat panel displays favor low haze transparent conductor for clear display effects. Despite the importance of haze for optoelectronic applications, conventional transparent conductors such as ITO thin films lack the tunability of haze because of their flat and homogeneous morphology. A broad range of light management layers have been developed to tune the haze of transparent conductors and improve solar cell and light-emitting diode performance.[13] However, implementing such additional layers in devices introduce extra processing steps and material cost. Studying the haze of on transparent conductors is imperative. Yet, there has only been one limited study on the haze of nanowire films so far, which compared the properties of two diameters of nanowires.[14] It is still not clear how to control

Dr. T. Gao, S. Haghanifar, M. I. Kayes, Z. Zhou, Prof. P. W. Leu
Department of Industrial Engineering
University of Pittsburgh
Pittsburgh, PA 15261, USA
E-mail: pleu@pitt.edu
M. G. Lindsay, B. D. Pafchek
Department of Mechanical Engineering
University of Pittsburgh
Pittsburgh, PA 15261, USA
Dr. P. Lu, Dr. P. R. Ohodnicki
National Energy Technology Laboratory
U.S. Department of Energy
Pittsburgh, PA 15236, USA
The ORCID identification number(s) for the author(s) of this article can be found under https://doi.org/10.1002/adom.201700829.

DOI: 10.1002/adom.201700829

haze in nanowire films, because the haze also depends on the nanowire film spacing, uniformity, alignment, and ordering, and there tends to be much randomness in these films.

In contrast to random metal nanowire films, we recently demonstrated metal nanomeshes that may be fabricated with well-defined morphology and high uniformity over large areas in any metal that can be deposited.[5] These metal nanomeshes have demonstrated comparable performance to ITO. The ability to fabricate metal nanomeshes with well-defined pitch, hole diameter, and thickness enables the engineering of particular optical properties such as transmission and haze.

In this paper, we evaluate the optical transmission, sheet resistance, and haze of metal nanomeshes as transparent conductors. We study these properties comprehensively through simulations for all nanomeshes with pitch and diameter less than 4000 nm and a thickness of 50 nm. The fundamental performance limits of these three properties are evaluated, and the tradeoffs between these three figures of merit as well as the correlations between these properties are discussed. In particular, a strong correlation between haze and transparency is found in nanomeshes. Metal nanomeshes with high transparency tend to have low haze and vice versa. Furthermore, we fabricate Cu nanomeshes with different geometries to verify our simulation results. The haze of metal nanomeshes may be primarily explained by Fraunhofer diffraction theory, and the spectral dependence of haze may be explained by Mie scattering from the metal regions between holes. In this paper, we focus on Cu nanomeshes, though the results of our studies should also apply to other metals. These results should also apply to all types of grating or grid-like structures, in which the metal structure has a well-defined 2D lattice.

2. Results and Discussions

Figure 1 shows a summary of our simulation results for metal nanomeshes. Figure 1a shows a schematic representation of the metal nanomesh, which consists of a metal thin film with cylindrical holes patterned in a hexagonal lattice. The morphology of metal nanomeshes is defined by the pitch of the hexagonal array a, the diameter of the holes d, and the thickness of the metal t. Figure 1b–d shows the sheet resistance R_s, total transmission at wavelength $\lambda = 550$ nm, and haze at $\lambda = 550$ nm, respectively, as a function of metal nanomesh pitch a and hole diameter d for nanomeshes with thickness $t = 50$ nm. The pitch a and hole diameter d range from 600 to 4000 nm, with $d < a$ to ensure continuity of the metal. The sheet resistance shown in Figure 1b was obtained through finite element analysis simulations and calculated as the average of $R_{s,xx}$ and $R_{s,yy}$, where $R_{s,xx}$ and $R_{s,yy}$ are the sheet resistance measured in the x- and y-directions, respectively. The simulations assume the bulk resistivity of Cu ($\rho = 1.68 \times 10^{-8}$ Ω m) and do not consider the polycrystallinity of the Cu or surface scattering of electrons. Thus, R_s should simply decrease linearly with increasing thickness in these simulations. The optical total transmission in Figure 1c accounts for the light scattered at all angles (both nonscattered and scattered) and will be referred to as the transmission, unless otherwise specified. The optical transmission

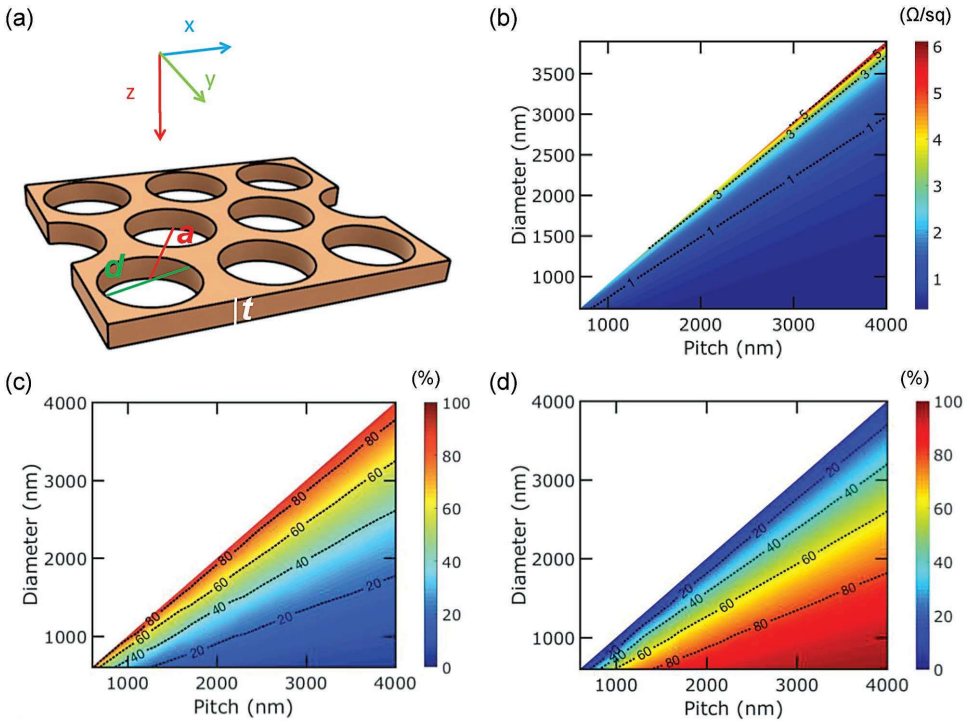

Figure 1. Simulated metal nanomesh properties. a) Metal nanomesh schematic representation. The metal nanomesh is defined by pitch a, hole diameter d, and thickness t. Contour plots of b) sheet resistance R_s of copper nanomeshes, c) transmission T (at $\lambda = 550$ nm), and d) haze H (at $\lambda = 550$ nm) as a function of pitch a and hole diameter d for thickness $t = 50$ nm.

was simulated by the finite-difference time-domain method with periodic boundary conditions.[15] Cu films are essentially opaque when thicker than 30 nm,[9] so the Cu nanomesh transmission should become approximately constant for thicknesses over 30 nm. The transmission is averaged for incident light polarized along the x- and y-directions with 550 nm wavelength. We find that a pitch greater than 1000 nm is needed for achieving transmission over 80%.

The haze H shown in Figure 1d is defined as

$$H = \frac{\text{Forward scattered light}}{\text{Total transmission}} \times 100\% \quad (1)$$

where the total transmission is equal to the sum of the forward nonscattered light and forward scattered light. The haze is computationally investigated by calculating the analytical Fraunhofer diffraction pattern of metal nanomeshes, where the metal nanomeshes are an infinite hexagonal array of cylindrical holes in an optically opaque film. The Fraunhofer diffraction pattern is calculated by sampling the diffraction pattern of a single hole (Bessel function of the first kind) at the k-points associated with the reciprocal lattice of the 2D hexagonal hole lattice. The (0, 0) diffraction mode is considered the forward nonscattered light, while the rest of the modes are considered forward scattered light. The haze calculated from this definition for the metal nanomeshes discussed in this paper is the same as the haze definition given by ASTM D1003,[16] where nonscattered forward light is considered as all transmitted light that deviates from the incident beam less than or equal to 2.5°, and scattered forward light is transmitted light that deviates from the incident beam greater than 2.5° ($\theta \leq 2.5°$ and $\theta > 2.5°$, respectively). Among all the Cu nanomeshes geometries in our study, the largest pitch is 4000 nm, corresponding to the lowest non-(0, 0) light mode diffracting at about 9° from the incidence angle. The lowest non-(0, 0) modes diffract at angles less than 2.5° only for $a \geq 14{,}600$ nm at $\lambda = 550$ nm.

Figure 2 plots the diffraction patterns of two different nanomeshes where θ is plotted on the radius from 0° to 90° and φ is plotted as the angle from 0° to 360°. θ is the angle of deviation from the incident beam along the z-axis or the zenith angle, and φ is the angle of rotation around the injection z-axis or azimuthal angle. Figure 2a plots the diffraction pattern of a nanomesh with pitch $a = 3500$ and $d = 3200$ nm and panel b plots the diffraction pattern with pitch $a = 1400$ and $d = 1000$ nm. These two particular nanomeshes were fabricated experimentally, and their experimental characterization will be discussed later and compared with simulation results. For the nanomesh with pitch $a = 3500$ nm, there are 109 modes present due to the large pitch. Since the holes are large, the light is mainly diffracted into the (0, 0) mode. As mentioned earlier, the (0, 0) diffraction mode is considered the forward nonscattered light, while the rest of the modes are considered forward scattered light. For this particular nanomesh, the analytical haze is 22% and from electrodynamic simulations, the transmission is 71% (compared to 76% from a geometrical shadowing calculation). Figure 2b plots the diffraction pattern of a metal nanomesh with pitch $a = 1400$ nm and diameter $d = 1000$ nm. Due to the smaller pitch, there are only 19 modes present. Since the holes are small, the light is also strongly diffracted into higher order modes, such that the haze is higher. The analytical haze is 49% and, from electrodynamic simulations, the transmission is 41% (compared to 46% from just a geometrical shadowing calculation).

In order to study the correlation between transmission, haze, and sheet resistance, we evaluated the range of values that are achievable by different nanomesh geometries. **Figure 3** plots the envelope or the range of transmission, haze, and sheet resistance for the metal nanomeshes simulated (specifically, 600 nm $\leq a \leq$ 4000 nm and 600 nm $\leq d \leq$ 4000 nm with $d < a$ and $t = 50$ nm). For different thicknesses above 30 nm, the haze and transmission should be about the same as those shown, since the Cu regions are essentially opaque, and for increasing thicknesses, the sheet resistance should decrease linearly. Figure 3a plots the range of transmission and haze (at $\lambda = 550$ nm). As can be seen from this plot, the transmission and haze show a strong and nearly linear correlation with each other. Nanomeshes with transmission $\geq$ 80% have $H \leq 17\%$ and nanomeshes with $H \geq$ 80% have transmission $\leq$ 21%. Figure 3b shows the range of sheet resistances and transmissions that are achievable. Cu nanomeshes with a higher transmission tend to have a higher sheet resistance, but increasing the thickness of the metal nanomesh may be utilized to

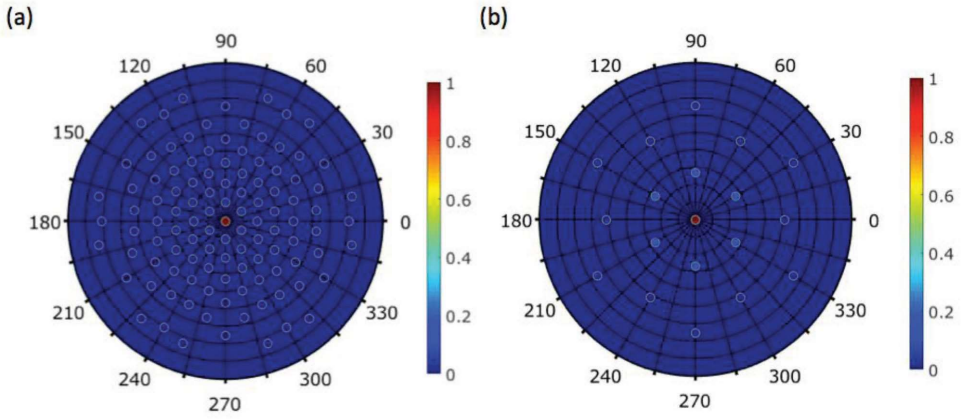

Figure 2. Diffraction patterns of different metal nanomeshes with a) $a = 3500$ and $d = 3200$ nm and b) $a = 1400$ and $d = 1000$ nm. The color scale shows light intensity normalized to the (0, 0) order diffraction mode.

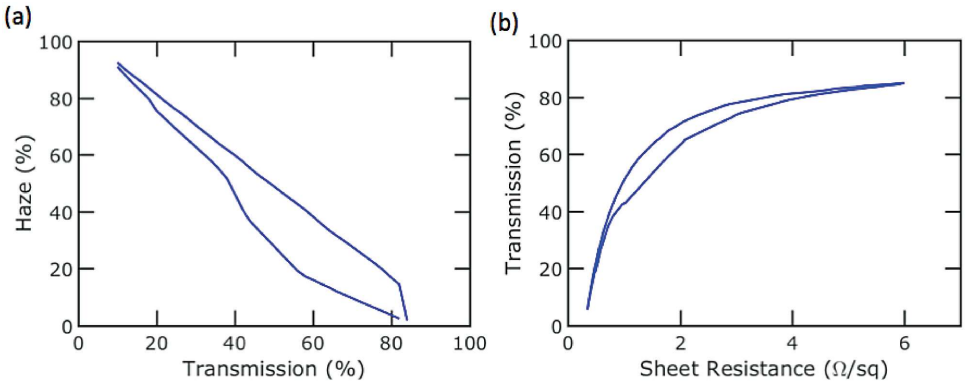

Figure 3. Performance limits of haze, transmission, and sheet resistance achievable in Cu nanomeshes of various hole diameters d and pitch a. The data shown are specifically for thickness $t = 50$ nm. a) Range of haze and transmission achievable by varying diameter and pitch. b) Range of transmission and sheet resistance.

decrease the sheet resistance without significantly sacrificing transmission. In addition, a variety of hierarchical structures have been reported to dramatically decrease sheet resistance and only slightly decrease transmission.[8,17]

We next studied the haze and transmission properties of various experimentally fabricated metal nanomeshes and compare them with simulation results. Cu nanomeshes of a variety of pitches and hole diameters with thickness $t = 50$ nm were fabricated by microsphere lithography.[5] **Figure 4** shows scanning electron microscope (SEM) pictures of two representative Cu nanomeshes at two different magnifications. The nanomeshes pictured have (a) $a = 3500$ and $d = 3200$ nm and (b) $a = 1400$ and $d = 1000$ nm, which are the same metal nanomeshes discussed specifically in simulations (Figure 2). We found that it is more difficult to fabricate larger pitch ($a = 3500$ nm) nanomeshes with high uniformity and ordering, because larger microspheres tend to have larger variance in diameter. The smaller pitch metal nanomesh also has some line defects and due to the longer etching times, the holes are slightly deformed or off center. The optical transmission was measured using a PerkinElmer Lambda 750 spectrophotometer. The transmission was measured with an integrating sphere, while the direct transmission was measured with a 2D optical detector. The transmissions for the samples shown in Figure 4a,b are 80% and 45%, respectively, at $\lambda = 550$ nm, compared with 71% and 41% from simulations discussed earlier. The hazes are 17% and 36%, respectively, at $\lambda = 550$ nm (compared to 22% and 49%, respectively, from theory) and the sheet resistances are 20 and 1.5 Ω sq^{-1}, respectively (compared to 2.6 and 0.9 Ω sq^{-1}, respectively, from simulations). The larger difference in sheet

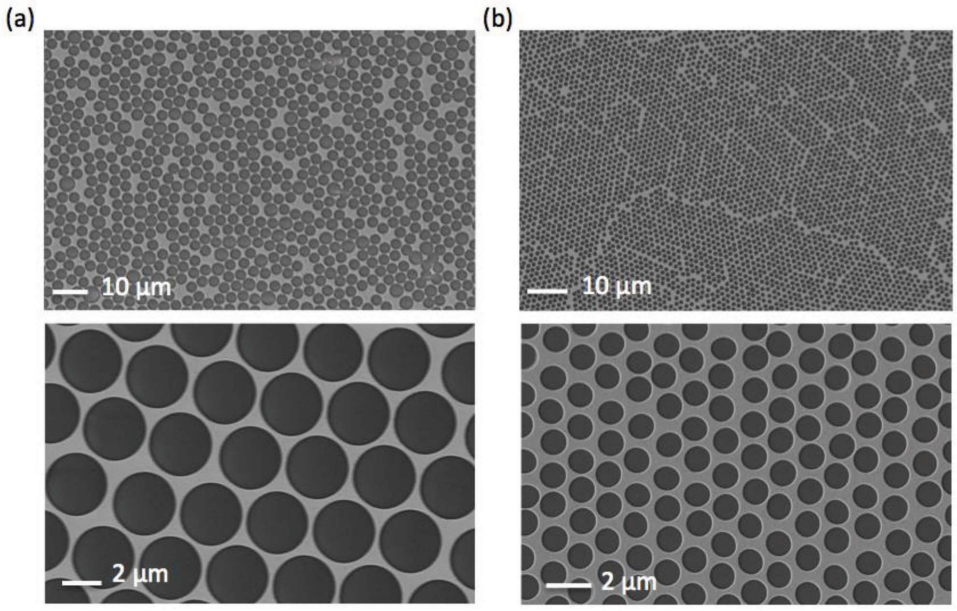

Figure 4. SEM pictures of Cu nanomeshes with different geometries fabricated using microsphere lithography. a) $a = 3500$ nm, $d = 3200$ nm and b) $a = 1400$ nm, $d = 1000$ nm. The thickness is 50 nm for both.

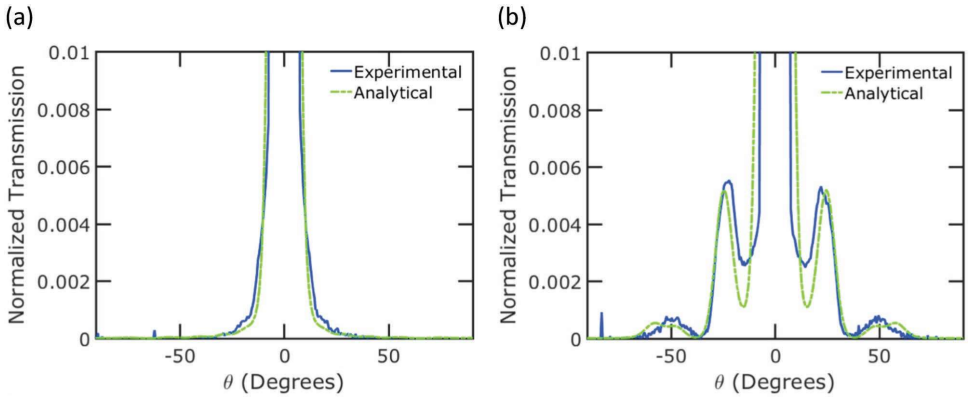

Figure 5. Angular distribution of normalized transmission through the Cu nanomeshes shown in Figure 4. a) a = 3500 nm, d = 3200 nm and b) a = 1400 nm, d = 1000 nm. The thickness is 50 nm for both.

resistance for the 3500 nm pitch nanomeshes may result from assumptions of bulk resistivity and some of the nonuniformity in experimental fabrication.

We next compared the angular distribution of the transmission through these Cu nanomeshes with analytical calculations. The angular distribution of transmission through the Cu nanomeshes was measured using a universal spectrometer (Cary 7000 Universal Measurement Spectrophotometer) with a 5 mm by 5 mm square beam at λ = 550 nm (**Figure 5**). The photodetector receives light in a 6° cone so that there is substantial broadening on the light intensities measured and the haze calculated directly from these plots has different values from that measured with an integrating sphere. The angular distribution was measured at two azimuthal angles, $\varphi = 0°$ and 180°, at varying zenith angle, $\theta = 0°$–90° to account for all transmission angles. Since the fabricated metal nanomeshes consist of various grains where the individual crystallites are oriented randomly, the diffraction modes are averaged over all φ and thus may still be observed. In addition to experimental data, we also plot the analytical solution for the metal nanomeshes assuming the size of the hole array is 5 by 5 in the case of the (a) larger pitch metal nanomesh and 9 by 9 in the case of the (b) smaller pitch metal nanomesh. The analytical data are also smoothed with a Gaussian kernel with a bandwidth of 3° to account for the photodetector receiving light over a 6° cone. As can be seen in Figure 5, the experimental and analytical data match well. While the larger metal nanomesh consists of many diffraction modes, most of the light is transmitted straight through into the (0, 0) mode. Since the higher modes are closely spaced together in angle and averaged over all azimuthal angles, the individual peaks are not observable. In contrast, for the smaller pitch metal nanomesh, the higher order diffraction modes can be observed. The experimental measured data appear to have broader higher order modes due to imperfections in the nanomesh crystal lattice (different sized holes, hole not being perfectly circular, off lattice site holes, etc.).

The hole spacing can be estimated from the width of the first-order diffraction modes using Bragg's law for a 2D hexagonal hole array.[18] The first-order diffraction, that is, first-order Debye ring, takes place when $a = \frac{2}{\sqrt{3}} \frac{\lambda}{\sin\theta}$. The maximum and minimum θ within the Debye ring correspond to the minimum and maximum of hole spacing a. The range of diffraction angle θ is obtained by peak fit. In Figure 5b, the center of the peak is at 23° and the full width at half maximum is 6.7°, with the 6° instrumental broadening subtracted. Therefore, the hole spacing is estimated to be ranging from 1430 to 1890 nm. The estimate is a result of the sum of all the aforementioned imperfection types.

Figure 6a shows the transmission and haze of all our fabricated Cu nanomeshes. By varying the pitch and hole diameter of the Cu nanomeshes, a variety of hazes ranging from 17% to 36%, and transmissions corresponding to 80–45% were measured. The experimentally measured values and correlation

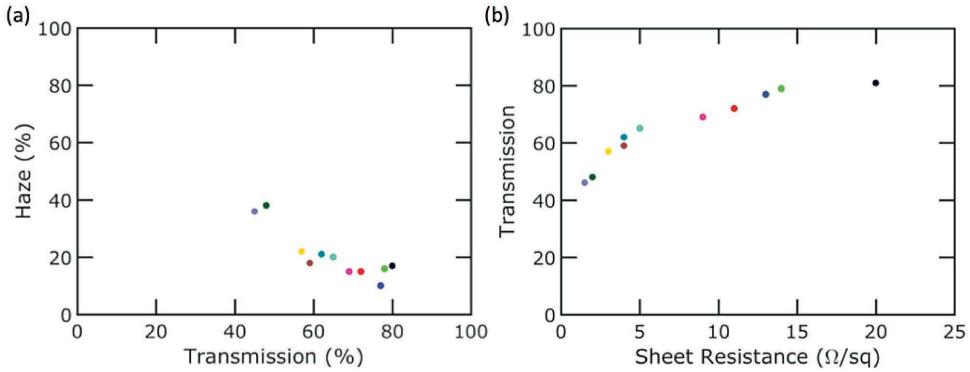

Figure 6. Range of a) transmission and haze, and b) sheet resistance and transmission from the fabricated Cu nanomesh samples.

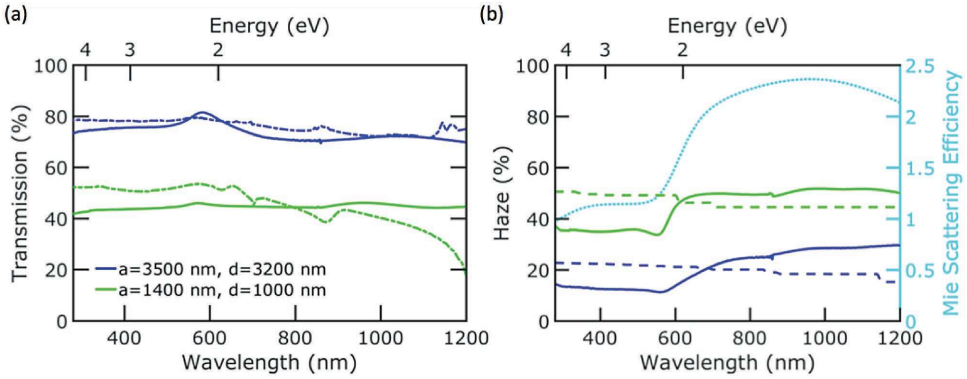

Figure 7. a) Transmission and b) haze as a function of wavelength for Cu nanomeshes with pitch $a = 1400$, diameter $d = 1000$ nm (green lines) and $a = 3500$ nm, $d = 3200$ nm (blue lines). The thickness is 50 nm for both nanomeshes. Experimental results are shown with solid lines and theoretical results are shown with dashed lines. The scattering efficiency of a single Cu nanowire with thickness $t = 50$ nm and width $w = 400$ nm is shown in (b) on the right *y*-axis in cyan.

match well with the computational results in Figure 3a. Smaller hole diameters are required by the Cu nanomeshes for a higher haze, which in turn compromise the transmission due to higher reflection and higher absorption. Figure 6b shows the sheet resistance and transmission of the fabricated nanomeshes. Cu nanomeshes with 80% transmission at 20 Ω sq^{-1} are demonstrated, which is comparable to ITO. Similar to the simulation results shown in Figure 3b, there is also a tradeoff between sheet resistance and transmission in the experimental data. The fabricated Cu nanomeshes exhibit higher sheet resistance than the simulation results at a fixed transmission, because our simulations assume bulk resistivity, ignore surface scattering, and assume ideal geometry.

Finally, we studied the transmission and haze as a function of wavelength. **Figure 7** shows the experimental and simulation results of (a) transmission and (b) haze as a function of wavelength for the same geometry nanomeshes that we have been discussing. The experimentally fabricated Cu nanomeshes have flatter transmission spectra compared with the simulation results because of their less perfect periodicity. The calculated haze spectra match the experimental results reasonably well for both geometries. The theoretical haze spectra decrease monotonically with increasing wavelength, as the number of diffraction modes decreases with increasing wavelength. For example, the large pitch ($a = 3500$ nm) nanomesh has 433 diffraction modes at $\lambda = 280$ nm and 19 modes at $\lambda = 1200$ nm and the smaller pitch ($a = 1400$ nm) nanomesh has 61 diffraction modes at $\lambda = 280$ nm and 7 modes at $\lambda = 1200$ nm. With less modes at larger wavelengths, more of the light intensity is concentrated in the (0, 0) nonscattered mode and thus the haze decreases. However, the experimentally measured haze tends to be lower at smaller wavelengths compared with the calculation. Instead of implementing metal properties in the haze calculation for nanomeshes, optically opaque material with zero reflection is assumed to provide a simple physical picture. The inflection points in the haze spectra near $\lambda = 550$ nm originate from the refractive indices of Cu. This discrepancy may be explained by Mie scattering from the metal regions between the holes. Figure 7b shows the Mie scattering efficiency of a single free-standing Cu nanowire with rectangular cross section, with thickness $t = 50$ nm, width $w = 400$ nm. This efficiency was calculated by the finite-difference time-domain method using a total-field scattered-field source to detect the scattered power flux. The Mie scattering efficiency of a Cu nanowire is defined as the ratio of the scattering cross section and the width of the nanowire w, where the scattering cross section is the energy flux removed from the incident light due to scattering. Mie scattering efficiency of Cu nanowire for incident light with electric field vector parallel and perpendicular to the nanowire was calculated respectively and averaged. As can be seen from the plot, this geometry has a lower Mie scattering efficiency at wavelengths shorter than 550 nm. The shape of the haze spectrum may be tuned by using different nanomesh materials, such as silver or gold.

3. Conclusions

In conclusion, we report both simulation and experimental results on transmission, sheet resistance, and haze of Cu nanomeshes. Simulations and theoretical calculations were used to comprehensively evaluate the transmission, haze, and sheet resistance of metal nanomesh structures, shedding light on the performance limits and correlation of metal nanomeshes as transparent conductors. Experimentally, we fabricated a variety of Cu nanomeshes to verify simulation results. The experimental results verify the correlation between haze and transmission. The haze may be primarily explained by Fraunhofer diffraction, though there are some Mie scattering effects from the metal region between holes. Future work will be devoted to breaking this correlation by introducing additional light-scattering elements to the Cu nanomesh.[19]

Acknowledgements

This work was supported by NSF grant #1552712. The authors thank Dr. David Pekker for helpful discussions.

Conflict of Interest

The authors declare no conflict of interest.

Keywords

diffraction, haze, metal nanomeshes, optoelectronics, transparent conductors

Received: August 5, 2017
Revised: January 26, 2018
Published online: March 8, 2018

[1] a) P. You, Z. Liu, Q. Tai, S. Liu, F. Yan, *Adv. Mater.* **2015**, *27*, 3632; b) J. van de Groep, D. Gupta, M. A. Verschuuren, M. M. Wienk, R. A. J. Janssen, A. Polman, *Sci. Rep.* **2015**, *5*, 11414; c) L. Kavan, P. Liska, S. M. Zakeeruddin, M. Grätzel, *Electrochim. Acta* **2016**, *195*, 34.

[2] a) T. H. Lee, K. H. Kim, B. R. Lee, J. H. Park, E. F. Schubert, T. G. Kim, *ACS Appl. Mater. Interfaces* **2016**, *8*, 35668; b) C. Song, N. Zhang, J. Lin, X. Guo, X. Liu, *Sci. Rep.* **2017**, *7*, 41250; c) L. Lian, D. Dong, S. Yang, B. Wei, G. He, *ACS Appl. Mater. Interfaces* **2017**, *9*, 11811.

[3] a) F. Cui, Y. Yu, L. Dou, J. Sun, Q. Yang, C. Schildknecht, K. Schierle-Arndt, P. Yang, *Nano Lett.* **2015**, *15*, 7610; b) D. Y. Choi, Y. S. Oh, D. Han, S. Yoo, H. J. Sung, S. S. Kim, *Adv. Funct. Mater.* **2015**, *25*, 3888; c) L. Dou, F. Cui, Y. Yu, G. Khanarian, S. W. Eaton, Q. Yang, J. Resasco, C. Schildknecht, K. Schierle-Arndt, P. Yang, *ACS Nano* **2016**, *10*, 2600.

[4] M. Mohl, A. Dombovari, R. Vajtai, P. M. Ajayan, K. Kordas, *Sci. Rep.* **2015**, *5*, 13710.

[5] T. Gao, B. Wang, B. Ding, J.-K. Lee, P. W. Leu, *Nano Lett.* **2014**, *14*, 2105.

[6] a) T. M. Barnes, X. Wu, J. Zhou, A. Duda, J. van de Lagemaat, T. J. Coutts, C. L. Weeks, D. A. Britz, P. Glatkowski, *Appl. Phys. Lett.* **2007**, *90*, 243503; b) D. S. Hecht, L. Hu, G. Irvin, *Adv. Mater.* **2011**, *23*, 1482; c) S. De, T. M. Higgins, P. E. Lyons, E. M. Doherty, P. N. Nirmalraj, W. J. Blau, J. J. Boland, J. N. Coleman, *ACS Nano* **2009**, *3*, 1767.

[7] a) P. Lee, J. Ham, J. Lee, S. Hong, S. Han, Y. D. Suh, S. E. Lee, J. Yeo, S. S. Lee, D. Lee, S. H. Ko, *Adv. Funct. Mater.* **2014**, *24*, 5671; b) C. S. Luo, P. Wan, H. Yang, S. A. A. Shah, X. Chen, *Adv. Funct. Mater.* **2017**, *27*, 1606339.

[8] a) T. Gao, Z. Li, P.-S. Huang, G. J. Shenoy, D. Parobek, S. Tan, J.-K. Lee, H. Liu, P. W. Leu, *ACS Nano* **2015**, *9*, 5440; b) T. Gao, P.-S. Huang, J.-K. Lee, P. W. Leu, *RSC Adv.* **2015**, *5*, 70713.

[9] T. Gao, P. W. Leu, *Opt. Express* **2013**, *21*, A419.

[10] a) T. Gao, P. W. Leu, *J. Appl. Phys.* **2013**, *114*, 063107; b) S. M. Bergin, Y.-H. Chen, A. R. Rathmell, P. Charbonneau, Z.-Y. Li, B. J. Wiley, *Nanoscale* **2012**, *4*, 1996.

[11] D. Ha, Z. Fang, L. Hu, J. N. Munday, *Adv. Energy Mater.* **2014**, *4*, 1301804.

[12] Y. Yao, J. Tao, J. Zou, B. Zhang, T. Li, J. Dai, M. Zhu, S. Wang, K. K. Fu, D. Henderson, E. Hitz, J. Peng, L. Hu, *Energy Environ. Sci.* **2016**, *9*, 2278.

[13] a) B. Wang, T. Gao, P. W. Leu, *Nano Energy* **2016**, *19*, 471; b) B. Wang, P. W. Leu, *Nano Energy* **2015**, *13*, 226.

[14] C. Preston, Y. Xu, X. Han, J. N. Munday, L. Hu, *Nano Res.* **2013**, *6*, 461.

[15] K. Yee, *IEEE Trans. Antennas Propag.* **1966**, *14*, 302.

[16] ASTM D1003-13, Standard Test Method for Haze and Luminous Transmittance of Transparent Plastics, **2013**, http://www.astm.org (accessed: January 2018).

[17] P.-C. Hsu, S. Wang, H. Wu, V. K. Narasimhan, D. Kong, H. Ryoung Lee, Y. Cui, *Nat. Commun.* **2013**, *4*, 2522.

[18] N. L. Smith, A. Coukouma, S. Dubnik, S. A. Asher, *Phys. Chem. Chem. Phys.* **2017**, *19*, 31813.

[19] S. Haghanifar, T. Gao, R. T. R. De Vecchis, B. Pafchek, T. D. B. Jacobs, P. W. Leu, *Optica* **2017**, *4*, 1522.